Wind Estimation for UAV Based on Multi-sensor Information Fusion

Gao Yanhui（高艳辉）[1*]，*Zhu Feifei*（朱菲菲）[2]，

Zhang Yong（张勇）[1]，*Hu Shousong*（胡寿松）[2]

1. Research Institute of UAV，Nanjing University of Aeronautics and Astronautics，Nanjing 210016，P. R. China；

2. College of Automation Engineering，Nanjing University of Aeronautics and Astronautics，Nanjing 210016，P. R. China

Abstract：Aiming at the requirements of accurate target positioning and autonomous capability for adapting to the environmental changes of unmanned aerial vehicle (UAV)，a new method for wind estimation and airspeed calibration is proposed. The method is implemented to obtain both wind speed and wind direction based on the information from a GPS receiver，an air data computer and a magnetic compass，combining with the velocity vector triangle relationships among ground speed，wind speed and air speed. Considering the installation error of Pitot tube，cubature Kalman filter (CKF) is applied to determine proportionality calibration coefficient of true airspeed，thus improving the accuracy of wind field information further. The entire autonomous flight simulation is performed in a constant 2-D wind using a digital simulation platform for UAV. Simulation results show that the wind speed and wind direction can be accurately estimated both in straight line and in turning segment during the path tracking by using the proposed method. The measurement accuracies of the wind speed and wind direction are 0. 62 m/s and 2. 57°，respectively.

Key words：wind estimation；airspeed calibration；unmanned aerial vehicle (UAV)；cubature Kalman filter (CKF)

CLC number：O321   **Document code**：A   **Article ID**：1005-1120(2015)01-0042-06

0   Introduction

Small and micro aerial vehicles are increasingly used to improve situational awareness by conducting surveillance，patrolling and convoy protection. Due to the inescapable fact that the low airspeed of unmanned aerial vehicles (UAVs) is comparable to the prevailing wind speed，constant wind and turbulence have a large impact on aircraft flight performance，energy consumption and aviation safety，specially for small and micro UAVs. Wise usage of wind information during navigation，such as thermal soaring and formation flight，can significantly increase the flight endurance of small UAVs. Sohn et al. [1] pointed out that such wind information could provide more accurate geo-location of a ground target. Additionally，the obtained crab-angle could help improve the control performance of a UAV in path following，landing tasks，etc. In fact，the wind estimation has become an important application of meteorological UAV[2].

Generally，the wind estimation for UAV can be roughly divided into three categories. The most widely used approach is graphical method based on the vector relationship among ground speed V_g，air speed V_a and wind speed V_w[3] as shown in Fig. 1，where ground speed is measured by radar or GPS，and air speed by a pitot tube and air data computer. Ref. [3] employed this method to calculate wind speed directly，circulating flight repeatedly to perform measurement calibration gradually by fixed airspeed of UAV. The second category is the constant wind estimation method using nonlinear Kalman filtering[4-5]，which adopts a nonlinear Kalman filter to conduct wind field estimation based on a constant wind
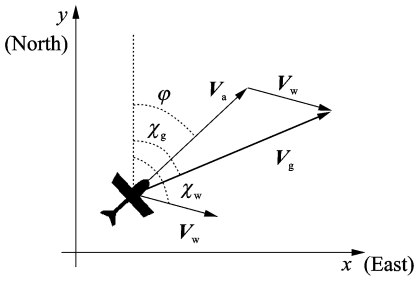
Fig. 1   Wind triangle

model without the reflection of abrupt change of wind velocity like wind gust. The third is the time-varying wind estimation method of non-Kalman filtering[6]. Wind speed is estimated according to measurement corrections, nonlinear kinetic equation, nonlinear wind model, and time-delayed moving average filter. But the method is limited to the numerous flight parameters, aerodynamic model and the case of a low speed aircraft such as a small UAV.

This paper proposes a new method for estimating wind speed and direction, using the measurement information outputting from a GPS receiver, the air data computer and magnetic compass. The proposed method also calibrates the airspeed scale factor that simplifies its application to low-cost UAVs. The method differs from previously used techniques in that it does not require a specific UAV flight maneuvers and can accurately estimate in straight line and turning segment during the trajectory following.

The implementation of wind estimation and airspeed calibration algorithm is first elaborated here. Subsequently the digital simulation platform for UAV is introduced briefly, along with the simulation results of wind estimation algorithm. Finally several conclusions are drawn.

1   Algorithm for Wind Estimation and Its Implementation

1.1   Algorithm for wind estimation

UAV flight kinematics satisfies the velocity vector triangle in the wind field, as shown in Fig. 1. Namely

$$\boldsymbol{V}_a = \boldsymbol{V}_g - \boldsymbol{V}_w \tag{1}$$

The Earth-fixed reference frame (FE) is selected for calculation. GPS receivers output the information of the ground speed $\boldsymbol{V}_g$, vertical velocity $\boldsymbol{V}_d$ and course angle χ_g in the FE. This paper mainly considers the 2-D constant wind model, which includes two parameters of wind speed and wind direction similarly using FE. The air data computer outputs airspeed in the flight-path reference frame (FW), therefore, the transformation from flight-path to body axes is required. Small UAV generally uses coordination turning flight, and the rudder is mainly used to eliminate sideslip angle, thus assuming $\beta \approx 0$. When the UAV is in a flight at a stable level, the formula $\alpha \approx \theta$ holds, thus

$$\boldsymbol{V}_a^{(n)} = \boldsymbol{V}_a \boldsymbol{C}_b^n \begin{bmatrix} \cos\alpha\cos\beta \\ \sin\beta \\ \sin\alpha\cos\beta \end{bmatrix} \approx \boldsymbol{V}_a \boldsymbol{C}_b^n \begin{bmatrix} \cos\theta \\ 0 \\ \sin\theta \end{bmatrix} \tag{2}$$

where the superscripts "n" and "b" denote the Earth-fixed and the body-fixed reference frames, respectively. $\boldsymbol{C}_b^n$ is the transformation matrix from the body-fixed reference frame to the Earth-fixed reference frame[7], namely

$$\boldsymbol{C}_b^n =$$
$$\begin{bmatrix} \cos\theta\cos\psi & \sin\phi\sin\theta\cos\psi - \cos\phi\sin\psi & \cos\phi\sin\theta\cos\psi + \sin\phi\sin\psi \\ \cos\theta\sin\psi & \sin\phi\sin\theta\sin\psi + \cos\phi\cos\psi & \cos\phi\sin\theta\sin\psi - \sin\phi\cos\psi \\ -\sin\theta & \sin\phi\cos\theta & \cos\phi\cos\theta \end{bmatrix} \tag{3}$$

Inserting the GPS information, wind condition, as well as Eqs. (2—3) into Eq. (1), an vector relationship can be yielded.

$$\boldsymbol{V}_a \begin{bmatrix} \cos^2\theta\cos\psi + \sin\theta(\cos\phi\sin\theta\cos\psi + \sin\phi\sin\psi) \\ \cos^2\theta\sin\psi + \sin\theta(\cos\phi\sin\theta\sin\psi - \sin\phi\cos\psi) \\ -\cos\theta\sin\theta + \cos\phi\cos\theta\sin\theta \end{bmatrix} =$$
$$\begin{bmatrix} \boldsymbol{V}_g\cos\chi_g \\ \boldsymbol{V}_g\sin\chi_g \\ \boldsymbol{V}_d \end{bmatrix} - \boldsymbol{V}_w \begin{bmatrix} \cos\chi_w \\ \sin\chi_w \\ 0 \end{bmatrix} \tag{4}$$

Generally speaking, the attack angle is small, for the sake of simplicity, assuming that $\sin\theta \approx 0$. In the 2-D horizontal plane, two equations can be obtained.

$$\boldsymbol{V}_a\cos^2\theta\cos\psi = \boldsymbol{V}_g\cos\chi_g - \boldsymbol{V}_w\cos\chi_w \tag{5}$$
$$\boldsymbol{V}_a\cos^2\theta\sin\psi = \boldsymbol{V}_g\sin\chi_g - \boldsymbol{V}_w\sin\chi_w \tag{6}$$

Calculating quadratic sum of Eqs. (5—6) yields

$$\boldsymbol{V}_a = \sqrt{\boldsymbol{V}_g^2 + \boldsymbol{V}_w^2 - 2\boldsymbol{V}_g\boldsymbol{V}_w\cos(\chi_w - \chi_g)} / \cos^2\theta \tag{7}$$

Airspeed $\boldsymbol{V}$ outputed from air data computer is calculated using the dynamic pressure and static pressure measured by a Pitot tube according to the Bernoulli's equation[4].

$$V_a^2 = \frac{2(P_t - P)}{\rho} \tag{8}$$

where P_t is the total pressure, P the static pressure, and ρ the air density.

The pressure measured by the head of airspeed tube and static pressure orifice is not exactly the same with the true value. Assuming that the attack angle of a pitot tube is small, the total pressure error measured by a pitot tube will be miniature. However, the static pressure error will be large. This is because the airflow near the static pressure orifice is disturbed due to the pressure sensor itself and the aircraft structure. Meanwhile, for the low-cost UAVs, the mounting position and orientation of a pitot tube may differ for each flight test leading to installation error changing greatly.

For the angle of attack if sideslip angle exists, the relationship between UAV airspeed and V_{pitot} can be expressed as follows

$$V_{pitot}^2 = |\boldsymbol{V}_a|^2 \cos\alpha\cos\beta \tag{9}$$

Therefore, the compensation factor sf is established aiming at the actual atmospheric environment, installation errors, attack and sideslip angle.

$$V_{pitot}^2 = sf^2 \cdot \frac{2(P_t - P)}{\rho} = sf^2 \cdot |\boldsymbol{V}_a|^2 \tag{10}$$

Substituting Eq. (7) into Eq. (9) gains

$$V_{pitot} = sf \cdot (\boldsymbol{V}_g^2 + \boldsymbol{V}_w^2 - 2\boldsymbol{V}_g\boldsymbol{V}_w\cos(\chi_w - \chi_g))/\cos^2\theta \tag{11}$$

Dividing Eq. (6) by Eq. (5), we have

$$\tan\psi = \frac{\boldsymbol{V}_g\sin\chi_g - \boldsymbol{V}_w\sin\chi_w}{\boldsymbol{V}_g\cos\chi_g - \boldsymbol{V}_w\cos\chi_w} \tag{12}$$

The heading angle range is $[0, 2\pi)$, while the range for arctangent function is $(-\frac{\pi}{2}, \frac{\pi}{2})$. Therefore, the four quadrant arctangent function $atan_2$ is chosen to calculate the heading angle. At the same time, conducting coordinate transformation by complementary operations, the formula can be expressed as

$$\psi = \mathrm{mod}(atan_2(\boldsymbol{V}_g\sin\chi_g - \boldsymbol{V}_w\sin\chi_w,$$

$$\boldsymbol{V}_g\cos\chi_g - \boldsymbol{V}_w\cos\chi), 2\pi) \tag{13}$$

The heading angle is measured by magnetic compass. The measurement of magnetic compass is the magnetic azimuth where the magnetic north direction uses the UAV longitudinal axis as a reference. The magnetic azimuth should be modified by a correction value (magnetic declination) in order to obtain the true azimuth of UAV longitudinal axis using the north direction as a reference. Assuming that magnetic declination in UAV flight area changes slightly, as long as conducting magnetic declination correction before the flight according to the take-off direction, the influences of magnetic declination angle on the precision of wind speed measurement can be ignored.

1.2 CKF algorithm

Recently proposed cubature Kalman filter (CKF) is a Gaussian approximation to Bayesian filter that could be used to solve a wide range of nonlinear filtering problems. The heart of the CKF is the third-degree spherical-radial cubature rule which makes it possible to compute the integrals encountered in nonlinear filtering problems. According to the spherical-radial cubature criterion, CKF calculates points with the same weight and diffuses them directly using nonlinear equations to conduct state estimation. With no need for linearization of nonlinear model, the estimation accuracy can reach three order. CKF performs better in nonlinear function approximation, numerical accuracy, and stability of the filter. In addition, the implementation is simple too[8-9].

Considering the multidimensional weighted integration as Eq. (14), the integral analytical value generally cannot be obtained, therefore it is necessary to select a group points (ω_i, ξ_i) with the weight to approximate the integral as Eq. (15).

$$I(f) = \int_{R^n} f(\boldsymbol{x})\exp(-\boldsymbol{x}^T\boldsymbol{x})\mathrm{d}\boldsymbol{x} \tag{14}$$

$$I(f) \approx \sum_{i=1}^m \omega_i f(\xi_i) \tag{15}$$

A CKF uses third-degree spherical-radial rule to generate the cubature-point set $\{\xi_i, \omega_i\}$ with the same weight when the dimension of the random variable is n.

$$\xi_i = \sqrt{\frac{m}{2}} [1]_i$$

$$\omega_i = \frac{1}{m}, i = 1, 2, \cdots; \ m = 2n \qquad (16)$$

After calculating cubature point set $\{\xi_i, \omega_i\}$, the CKF algorithm can be obtained based on time update and measurement update.

The time update step[10]

$$\boldsymbol{X}_{i,k-1|k-1} = \sqrt{\boldsymbol{P}_{k-1|k-1}} \xi_i + \hat{\boldsymbol{x}}_{k-1|k-1}$$

$$\boldsymbol{X}_{i,k|k-1}^* = f(\boldsymbol{X}_{i,k-1|k-1}, u_{k-1})$$

$$\hat{\boldsymbol{x}}_{k|k-1} = \frac{1}{m} \sum_{i=1}^{m} \boldsymbol{X}_{i,k|k-1}^*$$

$$\boldsymbol{P}_{k|k-1} = \frac{1}{m} \sum_{i=1}^{m} \boldsymbol{X}_{i,k|k-1}^* \boldsymbol{X}_{i,k|k-1}^{*\mathrm{T}} - \hat{\boldsymbol{x}}_{k|k-1} \hat{\boldsymbol{x}}_{k|k-1}^{\mathrm{T}} + \boldsymbol{Q}_{k-1} \qquad (17)$$

The measurement update step

$$\boldsymbol{X}_{i,k|k-1} = \sqrt{\boldsymbol{P}_{k|k-1}} \xi_i + \hat{\boldsymbol{x}}_{k|k-1}$$

$$\boldsymbol{Z}_{i,k|k-1} = h(\boldsymbol{X}_{i,k|k-1}, u_k)$$

$$\hat{\boldsymbol{z}}_{k|k-1} = \frac{1}{m} \sum_{i=1}^{m} \boldsymbol{Z}_{i,k|k-1}$$

$$\boldsymbol{P}_{zz,k|k-1} = \frac{1}{m} \sum_{i=1}^{m} \omega_i \boldsymbol{Z}_{i,k|k-1} \boldsymbol{Z}_{i,k|k-1}^{\mathrm{T}} - \hat{\boldsymbol{z}}_{k|k-1} \hat{\boldsymbol{z}}_{k|k-1}^{\mathrm{T}} + \boldsymbol{R}_k$$

$$\boldsymbol{P}_{xz,k|k-1} = \frac{1}{m} \sum_{i=1}^{m} \omega_i \boldsymbol{X}_{i,k|k-1} \boldsymbol{Z}_{i,k|k-1}^{\mathrm{T}} - \hat{\boldsymbol{x}}_{k|k-1} \hat{\boldsymbol{z}}_{k|k-1}^{\mathrm{T}}$$

$$\boldsymbol{W}_k = \boldsymbol{P}_{xz,k|k-1} \boldsymbol{P}_{zz,k|k-1}^{-1}$$

$$\hat{\boldsymbol{x}}_{k|k} = \hat{\boldsymbol{x}}_{k|k-1} + \boldsymbol{W}_k (\boldsymbol{z}_k - \hat{\boldsymbol{z}}_{k|k-1})$$

$$\boldsymbol{P}_{k|k} = \boldsymbol{P}_{k|k-1} - \boldsymbol{W}_k \boldsymbol{P}_{zz,k|k-1} \boldsymbol{W}_k^{\mathrm{T}} \qquad (18)$$

1.3 Wind estimation algorithm implementation

With the assumption of a constant 2-D wind, a CKF method is suggested to estimate the wind speed, wind direction and airspeed calibration coefficient simultaneously. These variables can be regarded as constant approximately during some flight time. The states are modeled as a random-walk process[4].

With the state vector $\boldsymbol{x} = [\boldsymbol{V}_w \quad \chi_w \quad sf]^{\mathrm{T}}$, the system dynamics is described by Eq. (19)

$$\boldsymbol{x}(k+1) = \boldsymbol{F}\boldsymbol{x}(k) + w_k \qquad (19)$$

where $\boldsymbol{F}$ is the unit matrix and $w \sim N(0, \boldsymbol{Q}_k)$.

The ground velocity and the course angle, both of which are outputs of the GPS receiver, and the pitch angle measured from vertical gyroscope are accurate enough to be treated as known parameters in each epoch. With the measured variables $\boldsymbol{z}_k = [\boldsymbol{V}_a \quad \psi]$, the nonlinear observation equation is expressed as

$$\boldsymbol{z}_k = \begin{bmatrix} sf \cdot (\boldsymbol{V}_g^2 + \boldsymbol{V}_w^2 - 2\boldsymbol{V}_g\boldsymbol{V}_w\cos(\chi_w - \chi_g))/\cos^2\theta \\ \psi \end{bmatrix} + \boldsymbol{v}_k \qquad (20)$$

where $\boldsymbol{v}_k \sim N(0, \boldsymbol{R}_k)$, and ψ is described by Eq. (13).

In the simulations, the measurement and the process noise covariance are tuned using real flight test results. The initial guess at the wind vector is obtained by calculating the velocity vector triangle.

2 Simulation and Verification

2.1 Simulation platform

This section is devoted to the simulation analysis for characterizing the performance of the CKF developed in Section 1. The filter has been tested with the simulated flight data provided by a certain UAV digital simulation platform[11-12]. The controller of a certain UAV employs the method of classical proportional differential (PD) control, which comprises of an inner loop and an outer loop. The autonomous navigation algorithm uses lateral offset and the rate of lateral offset directly to calculate given roll angle for autonomous flight guidance.

2.2 Simulation results

It is assumed that the initial value of the calibration coefficient is approximately 10% smaller than the true value. The wind speed and the wind direction are set to 30 m/s and 32.45°, respectively. The measurement noise covariance of the airspeed is chosen as the variance of measurements obtained from the air data computer, and the measurement noise covariance of the heading angle as the variance of measurements obtained from the magnetic compass. The measurement noise is modeled as zero-mean colored noise. The noise characteristics are obtained from test flight data. The parameters for CKF used in simulation include: the initial covariance $\boldsymbol{P}_0 = \begin{bmatrix} 15^2 & 0 & 0 \\ 0 & \pi^2 & 0 \\ 0 & 0 & 0.3^2 \end{bmatrix}$,

the measurement noise $\boldsymbol{R} = \begin{bmatrix} 6 & 0 \\ 0 & 10^{-3} \end{bmatrix}$, and the

process noise covariance $Q =$

$$\begin{bmatrix} 2\times10^{-5} & 0 & 0 \\ 0 & 3.5\times10^{-8} & 0 \\ 0 & 0 & 3\times10^{-7} \end{bmatrix}.$$

The UAV conducted the entire autonomous flight simulation on a digital simulation platform. The vehicle was flying over a preplanned sequence of waypoints. The constant wind disturbance was created at the level flight. The angle between the directions of direct crosswind and airline in level flight segment was 90°. This was almost the worst case with respect to the initial value guesses. The CKF filter started to work after UAV achieved a steady flight. The estimation results of wind speed, wind azimuth, and scaling factor of airspeed calibration were shown in Fig. 2. The associated estimation errors were shown in Fig. 3.
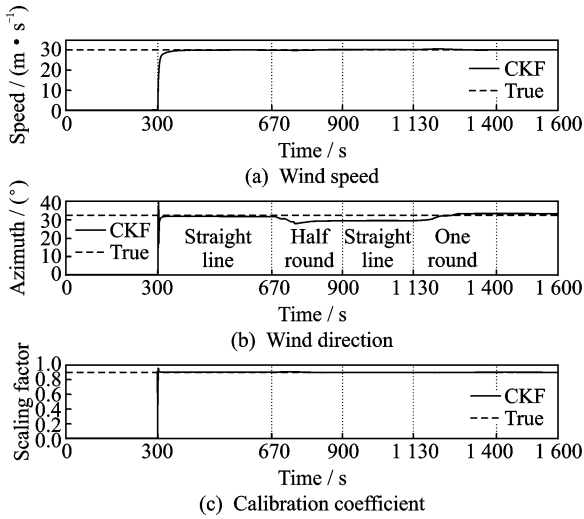

Fig. 2   Simulation results of wind speed, wind direction and calibration coefficient

From Figs. 2,3, the CKF estimation switched automatically in 300 s. The whole flight process can be divided into four phases: the phase of straight line (300—670 s), the phase of a half of round turn (670—900 s), the phase of straight line (900—1 130 s), and the phase of a round turn (1 130—1 400 s). In the UAV straight line autonomous flight process, the wind speed and calibration coefficient can be predicted rapidly. From Fig. 2(a) and Fig. 3(a), the wind speed residual is less than 0.5 m/s during the whole estimation process. From Fig. 2(b) and Fig. 3(b), the wind direction residual is less than 3° after a
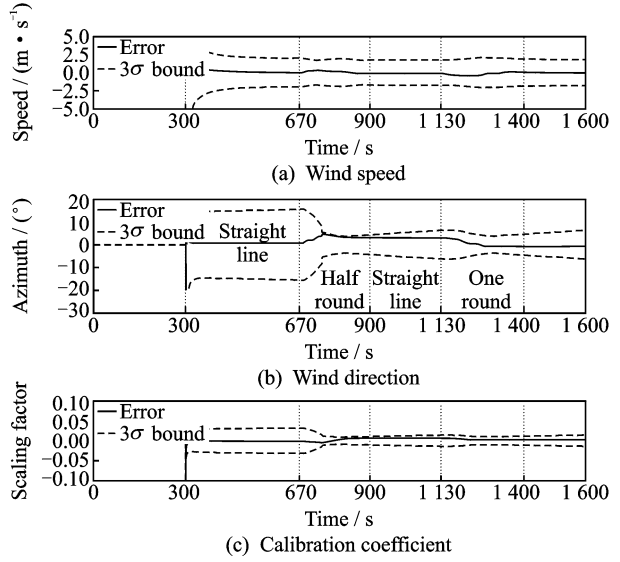

Fig. 3   Simulation results of residuals with 3σ bounds

semicycle flight, and the wind direction residual is less than 1° after a round flight. Furthermore, from Fig. 2(c) and Fig. 3(c), the calibration coefficient residual is less than 0.006. The estimation results of the wind speed, wind direction and calibration coefficient all satisfy the residual requirements of 3δ bound. And it shows that the CKF estimation results are credible.

As an objective measure of the CKF estimation method is preferable, the average of the root mean squared error (δ) is calculated for different flight segment

$$\delta = \sqrt{\frac{1}{n}\sum(t_i - s_i)^2} \qquad (21)$$

where t is the truth-value and s the value of simulation.

The results of the performed estimations in different flight segments are summarized in Table 1, where the unreported accuracies are left blank. Also, the CKF wind component observations are compared with accuracies of conventional atmospheric profiling systems such as atmospheric wind profiler, radiosondes and meteorological UAV.

In Table 1, the measuring precision of wind field information estimated by CKF method is superior to the traditional wind measurement equipments. The convergence time of filtering is the flight time of semicycle, and the measurement accuracies of wind speed and wind direction are 0.62 m/s and 2.57°, respectively.

Table 1   Comparison of accuracies for wind component observations

Wind estimation method		Wind speed/ $(m \cdot s^{-1})$	Wind direction/ $(°)$
Atmospheric wind profiler[13]		2	
Vaisala RS92 radiosonde[14]		1	15
Aerosonde UAV[15]		1	
CKF	After 300 s	0.96	6.7
	After half round	0.62	2.57
	After one round	0.48	1.6

3   Conclusions

A new method is presented for estimating wind speed and direction as well as for calibrating the airspeed using GPS receiver，air data computer，magnetic compass and vertical gyroscope. The proposed algorithm uses the geometrical relation of ground，wind speed and airspeed，which does not depend on aerodynamic model. The simulation results show that the recommended CKF estimation method can obtain reasonable wind speed，wind direction information only within a round of UAV autonomous turn flight. The estimated scaling factor also corrects the airspeed to a reasonable level. The wind speed and wind direction of UAV in current airspace can be acquired by the proposed method in real-time，which contributes to the more accurately location and time predication of task-performing for commanders. Therefore，the method is conducive to complete operational mission synergistically. Simultaneously，the method provides research foundation for the subsequent UAV real-time path planning in wind fields.

Acknowledgement

References：

[1]   Sohn S，Lee B，Kim J，et al. Vision-based real-time target localization for single-antenna GPS-guided UAV[J]. IEEE Transactions on Aerospace and Electronic Systems，2008，44(4):1391-1401.

[2]   Buschmann M，Bange J，Vörsmann P. MMAV-A miniature unmanned aerial vehicle (MINI-UAV) for meteorological purposes[C] // 16th Symposium on Boundary Layers and Turbulence. Portland，United states：American Meteorological Society，2004：263-269.

[3]   Hollister W M，Bradford E R，Welch J D. Using aircraft radar tracks to estimate winds aloft[J]. MIT Lincoln Laboratory Journal，1989(2):555-565.

[4]   Cho A，Kim J，Lee S，et al. Wind estimation and airspeed calibration using a UAV with a single-antenna GPS receiver and pitot tube[J]. IEEE Transactions on Aerospace and Electronic Systems，2011，47(1):109-117.

[5]   Pachter M，Ceccarelli N，Chandler P. Estimating MAV's heading and the wind speed and direction using GPS，inertial，and air speed measurements[C] // AIAA Guidance，Navigation and Control Conference and Exhibit. Honolulu，USA：AIAA，2008:1-25.

[6]   Langelaan J W，Alley N，Neidhoefer J. Wind field estimation for small unmanned aerial vehicles[J]. Journal of Guidance，Control，and Dynamics，2011，34(4):1016-1030.

[7]   Phillips W F. Mechanics of flight[M]. 2nd Ed. Hoboken，USA：John Wiley & Sons，Inc，2010.

[8]   Gu Dongqing，Qin Yongyuan，Peng Rong，et al. Rapid transfer alignment using federated Kalman filter[J]. Transactions of Nanjing University of Aeronautics and Astronautics，2005，22(2)：139-143.

[9]   Liu Lin，Li Hui，Dai Beiqian，et al. Speech enhancement method based on Kalman filtering and multi-pluse excitation[J]. Journal of Data Acquisition and Processing，2009，24(1):100-104.

[10] Arasaratnam I，Haykin S. Cubature Kalman filters[J]. Automatic Control，IEEE Transactions on，2009，54(6):1254-1269.

[11] Gao Yanhui，Xiao Qiangui，Hu Shousong，et al. Flight control system simulation platform for UAV based on integrating simulink with stateflow[J]. Telkomnika-Indonesian Journal of Electrical Engineering，2012，10(5):985-991.

[12] Liu Rong，Lu Yuping，Xiao Qiangui. Low-cost and super-applicability digital navigation and control system of super-size UAV[J]. Journal of Nanjing University of Aeronautics & Astronautics，2009，41(S):19-23.

[13] Sun Xuying，Han Hui，Duan Haixia，et al. Comparative analysis on wind data from atmospheric wind profiler and balloon sounding[J]. Arid Meteorology，2008，26(3):48-52.

[14] Li Wei，Xing Yi，Ma Shuqing. The analysis and comparison between GTSl radiosonde made in China and RS92 radiosonde of Vaisala Company[J]. Meteorological Monthly，2009，32(10):97-102.

[15] Soddell J R，McGuffie K，Holland G J. Intercomparison of atmospheric soundings from the aerosonde and radiosonde[J]. Journal of Applied Meteorology，2004，43(9):1260-1269.

(Executive editor：Zhang Tong)